Environ Monit Assess (2024) 196:398
https://doi.org/10.1007/s10661-024-12523-3

RESEARCH

Geochemical, mineralogical records, and statistical approaches in establishing sedimentary in the environment of a Mediterranean coastal system: case of Sebkha El-Guettiate (southeastern Tunisia)

Najia Bouabid · Feyda Srarfi · Hayet Mnasri · Mohamed Ali Tagorti

Received: 20 October 2023 / Accepted: 5 March 2024 / Published online: 26 March 2024

Abstract The current study was conducted within the context of the Holocene era in Sebkha El-Guettiate, located in southeastern Tunisia. The aim was to determine the factors influencing the geochemical and mineralogical composition of sediments and to elucidate the sedimentary characteristics of the Holocene within the Sebkha core. We examined a sediment core extending 100 cm from this Sebkha, subjecting it to comprehensive analysis to uncover its sedimentological, mineralogical, and geochemical properties. Several techniques were employed to strengthen and validate the connections between geochemical and mineralogical analyses, including X-ray diffraction (XRD), X-ray fluorescence (XRF), scanning electron microscopy (SEM), and infrared (IR) spectroscopy, among others. Furthermore, statistical analyses utilizing principal component analysis (PCA) were applied to the results of the geochemical and mineralogical studies, aiding in the identification of patterns and relationships. A comprehensive mineralogical assessment of the core's sediments revealed the presence and interpretation of carbonate minerals, evaporite minerals, and detrital minerals. Through the application of infrared (IR) spectrometer techniques to all sediment samples, we gained insight into the mineralogical components and the distribution of key elements such as quartz, kaolinite, calcite, feldspar, and organic carbon. The geochemical composition demonstrated a clear dominance of silica (SiO2), accompanied by fluctuations in carbonate percentages (CaCO3). The prominent major elements, primarily magnesium (Mg) and calcium (Ca) originating from dolomitization, sodium (Na) and chlorine (Cl) from halite, and calcium (Ca) from gypsum, exhibited varying levels. Results from Rock–Eval 6 pyrolysis indicated that the organic matter within the sediments is generally a mixture of terrestrial and aquatic origins. This study provides practical information that underscores the diverse origins contributing to Sebkha sediment formation, often influenced by saline systems.

Keywords Geochemistry · Mineralogy · Sedimentary · Sebkha El-Guettiate · Southeast Tunisia

N. Bouabid (✉) · H. Mnasri
Higher Institute of Water Sciences and Techniques of Gabès (ISSTEG), University of Gabès, Gabès, Tunisia
e-mail: bouabidnajia@yahoo.fr

N. Bouabid · H. Mnasri
Research Laboratory Geo-Systems, Geo-Resources, Geo-Environment (LR3G), Department of Geology, Faculty of Sciences of Gabès, University of Gabès, City Campus Erriadh-Zrig, 6072 Gabès, Tunisia

F. Srarfi
Research Laboratory L3G (LR18ES37), Faculty of Science of Tunis, El Manar University, 1060 Tunis, Tunisia

M. A. Tagorti
Research Laboratory: Minerals Resources and Environment, Department of Geology, Faculty of Sciences of Tunis, University of Tunis El Manar (LR01ES06), Tunis, Tunisia

Introduction

Coastal zones encompass a diverse range of activity sectors, with sediment transport holding a significant role within the environmental context. In the Mediterranean region, paleoclimatic records distinctly reveal that the Holocene era is characterized by millennial-scale climatic fluctuations. These variations are closely tied to shifts in temperature and fluctuations in rainfall, which are prominently evident during this period (e.g., Bond et al., 2001; Mayewski et al., 2004; Magny, 2004; Giraudi, 2005; Wanner et al., 2008; Magny et al., 2011; Giraudi et al., 2011; Arnaud et al., 2012; Benito et al., 2015; Al-Hurban et al., 2023). The African Mediterranean climate demonstrates a notable diversity in its climatic systems, ranging from humid equatorial conditions to arid seasonal tropical climates and subtropical climates. In fact, increasing temperatures across Africa are anticipated to elevate evaporation demands (Goulden et al., 2009).

Indeed, rising temperatures across Africa are expected to increase evaporation demands (Bedair et al., 2023; Terink et al., 2013). Furthermore, the regional climates in Africa have undergone significant changes since the last glacial maximum, approximately 21,000 years ago (Wanner et al., 2008; Armstrong et al., 2023). These transformations have been documented through pollen syntheses, illustrating notable shifts. Understanding the complex history of past climatic changes and their effects remains a challenge. Notably, exceptional records based on charcoal and pollen proxies have shed light on anthropogenic influences (Jaouadi et al., 2016; Marquer et al., 2008; Nash & Meadows, 2012; Schulz et al., 2002). In recent years, the Tunisian coast has garnered increased attention within the environmental context (Zaîbi et al., 2011, Zaibi et al., 2012, Zaïbi et al., 2016; Gargouri and Zouari, 2019; Gammoudi et al., 2021). Over the past two millennia, despite the expansion of Sebkha basins at the expense of agricultural lands, industrial zones, and urban areas in Tunisia, records have provided limited insights into the finer fluctuations of temperature and humidity.

According to Lakhdar et al., (2021), the southern coast of Tunisia is characterized by subtle tides that reach their peak in the Gulf of Gabes, renowned in the Mediterranean for its tide oscillations. The southeastern Tunisian coastal zone features the presence of Sebkhas or salt flats. Multiple studies have established that climatic changes during the Holocene period were numerous, although less pronounced in their variations compared to those during the preceding glacial cycle (Chairi, 2005; Jaouadi et al., 2016; Lakhdar et al., 2006; Schulz et al., 2002; Zaibi et al., 2012). However, the Holocene coastal deposits hold crucial insights into the evolution of successive paleoenvironments, regional hydrodynamic influences, tectonic activities, and hydro-isostatic responses of the littoral fringe to sea-level fluctuations (Zaîbi et al., 2011; Engel et al., 2021). In Sebkhas, the effects of wind deflation add another layer of complexity, at times quite vigorous and capable of altering the topographic landscape.

The research area, situated in the southeastern region of Tunisia, appears to have witnessed the establishment of an estuarine open lagoon environment around 7460 calendar years BP. Subsequent to this phase, several periods of sedimentation interruptions occurred, leading to the formation of sandy ridges, particularly around 5408 calendar years BP. These episodes have contributed to shifts in paleoenvironments, leading to the transformation of increasingly enclosed lagoons that eventually evolved into the present-day Sebkha environment (Zaîbi et al., 2011). The region has been the subject of extensive investigation (Zaîbi et al., 2011, Zaibi et al., 2012, Zaïbi et al., 2016; Gargouri and Zouari, 2019).

This study's primary objective is to elucidate the sedimentary characteristics of the Holocene within the Sebkha core. The aim is to discern the origin of minerals and provide insights into the source and nature of organic matter. By examining variables such as carbonate percentage, chemical elements, organic content, and granulometric distribution, one can deduce variations in the climatic conditions of deposition environments. In order to reinforce and validate the connections between geochemical and mineralogical analyses, a variety of techniques, including principal component analysis (PCA), were utilized, encompassing processes such as X-ray diffraction (XRD), X-ray fluorescence (XRF), scanning electron microscopy (SEM/EDX), and infrared (IR) spectroscopy, among others.

In the present study, we examine the sources, composition, and evolution of organic matter (OM) in the recently deposited sediments of the Sebkha El-Guettiate using Rock–Eval 6 (RE) parameters and inorganic analysis to assess the types of inorganic and organic inputs in the core, to discuss the results of

RE parameters and the geochemical proxy data, and to determine the source and state of organic matter preservation in the Sebkha environment. But, these are preliminary results that can be supplemented by a further micro-morphological assessment and more involvement in pedo-sedimentary events.

Study area

The study area, with a rectangular shape, is situated along the coastal fringes of Southeast Tunisia, specifically within the Gulf of Gabes in the southwestern Mediterranean region. Tunisia, showcasing a wide bioclimatic range, covers a total area of 518 km^2 within coordinates of 34°13′48″N and 10°03′06″E (Fig. 1). This region is characterized by an arid climate and is positioned approximately 15 km to the south of Skhira city.

The Skhira coastal region within the central part of the Gulf of Gabes displays a distinctive morphology that varies proportionally. Progressing from north to south, the coastline is marked by a commanding cliff ranging from 1 to 15 m in height. This cliff is followed by a paralic system consisting of two maritime marshes, namely El-Guettiate and Dreïaa. These marshes are sheltered by a cliff and a narrow sandy rim (Gargouri, 2011).

In contrast, the northern section of the Sebkha is adjacent to the Mediterranean, separated by a narrow strip of land. This strip occasionally unveils an elongated cliff, stretching over 2 km in length and spanning 100 to 200 m in width. This northern cliff transitions to the south, transforming into a barrier beach system reminiscent of sand spits that extend for 2 km (Zaîbi et al., 2011). The connection between the Mediterranean Sea and the Sebkha occurs primarily through a tidal channel on the eastern side. This channel measures 10 m in width and reaches depths of up to 7 m. The Sebkha El-Guettiate serves as an outlet for the Bou Saïd and El Ghram wadis, which collectively have a catchment area estimated at 378.2 km^2 (Fig. 1).

Methods and materials

During the field expedition, a sediment core measuring 100 cm in length (SG: 34°12′14.45″N; 10°04′28.27″E) was collected from the Sebkha El-Guettiate, as depicted in Fig. 1. This core was sampled at intervals of 0.5 cm, yielding a total of 200 samples. Subsequently, eleven samples were carefully selected, maintaining a 10-cm interval between each, for the purpose of conducting geochemical and mineralogical analyses.

The examination of the mineralogical composition of the fine fraction was carried out through X-ray diffraction (XRD) analysis.

This analysis involved utilizing raw sample powders to identify phases. The XRD analysis took place at the Laboratory of Nanomaterials and Systems for Renewable Energies within the Energy Research and Technology Center (CRTEn) in Borj Cedria, Tunisia. This component encompassed a comprehensive mineralogical analysis of the entire rock and clays using the X-ray diffraction method. Its purpose was to determine the mineralogical composition of the sediment samples that were collected.

X-ray diffractograms were generated using the X'Pert High Score Plus software. The software then compared the resulting diffractograms with the nearest available reference files to discern the mineralogical composition. In summary, the field expedition yielded a sediment core from Sebkha El-Guettiate, and subsequent analyses involved careful selection of samples for geochemical and mineralogical investigations. X-ray diffraction (XRD) analysis was conducted on fine fraction samples to identify mineral phases.

Based on the mineralogy of the whole rock, some samples were subjected to SEM (scanning electron microscope) at the Tunisian Company of Petroleum Activities (ETAP) observations to determine the texture of the figurative elements. Again, the infrared (IR) technique complements X-ray diffraction analysis in the study of poorly crystallized materials. This method of analysis is non-destructive for the sample. The measurements were carried out by transmission. The device used is a dispersive infrared spectrometer of the PerkinElmer brand. The pellets were made from an intimate mixture of 1 mg ground sample and with 100 mg of potassium bromide (KBr) under a pressure of 4.5 110 Pa. To determine the percentages of CaCO3, the Denard Calcimeter is used. But, major and minor chemical elements were measured by XRF spectrometer, and the concentrations of potassium (K) and sodium (Na) were measured by flame photometer for 200 samples at the Valorization of Useful Materials Laboratory (LVMU) of the National Research Center in Materials Science (CNRSM), Borj Cedria, Tunisia. However, the organic matter analyses used

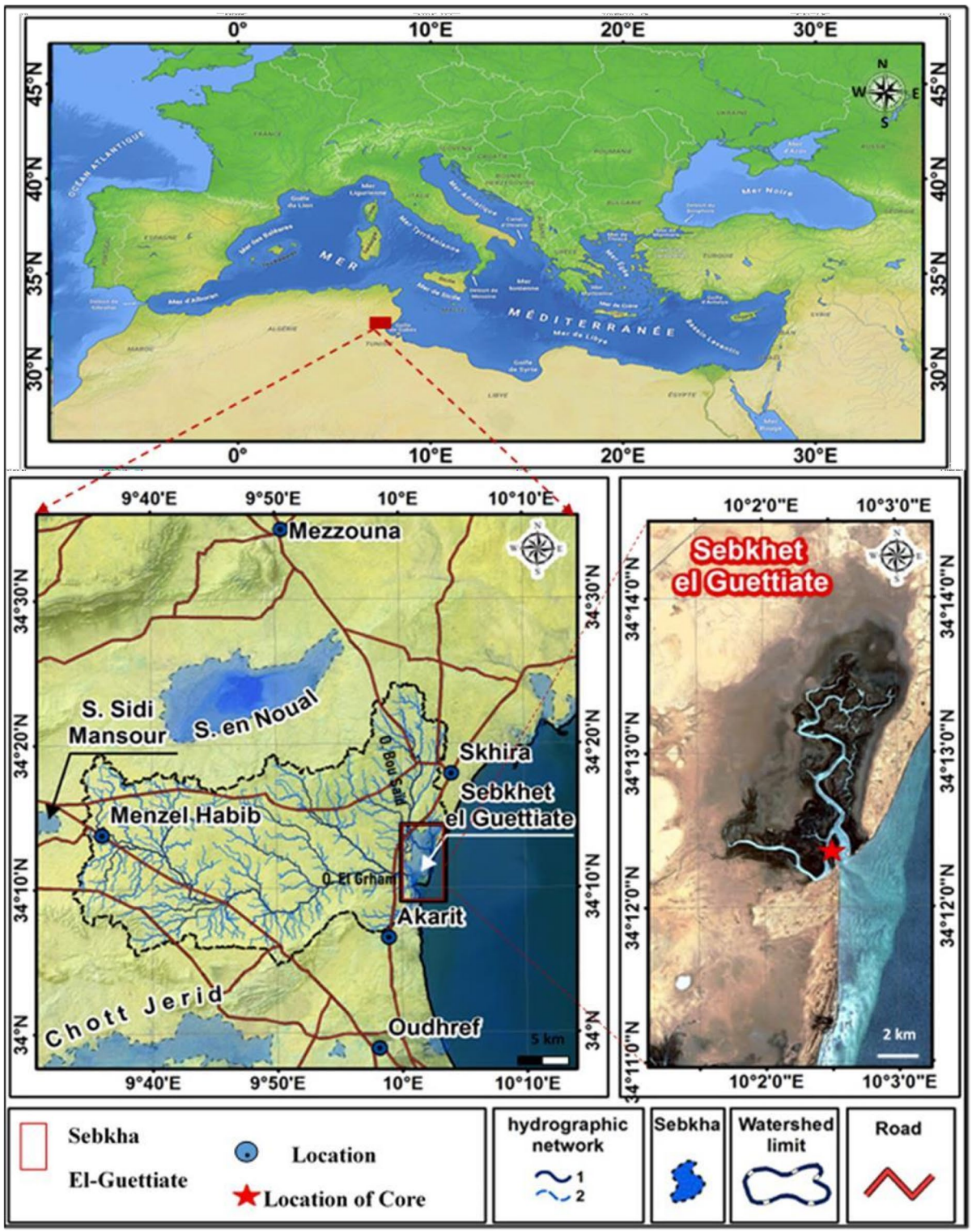

Fig. 1 Location of the Sebkha of El-Guettiate within the framework of a Mediterranean and Atlantic connection, limit of the catchment area of the study area, and location of the core taken from SG

the Rock–Eval 6 at the Tunisian Company of Petroleum Activities (ETAP). For statistical data processing, the statistical software XLSTAT 2023 was used.

Results

Sedimentology and mineralogy studies

In the process of examining and comprehending the arrangement of essential sediment layers within the Sebkha El-Guettiate (depicted in Fig. 2), it is observed that the proportion of finer sediment particles (< 63 µm) fluctuates between 19 and 69.8%. Furthermore, the computation of the proportion attributed to coarser particles, with diameters surpassing 63 µm, ranges from 8 to 28%. Notably, the particle size analysis of this core reveals a considerable variance in the proportions of sandy and silty components. However, the examination of the mineral composition within Sebkha El-Guettiate reveals distinctive diffractograms in the sediments of the SG core, extracted from depths of 20 cm and 80 cm. These diffractograms unveil a specific arrangement of minerals, including silicates (quartz, feldspar, and phyllosilicates), carbonates (calcite, dolomite, magnesium, and Ankerite), and evaporites (gypsum and halite), as illustrated in Fig. 3. Notably, these findings are characterized by the proportional presence of various minerals, as outlined in Table 1. These percentages accentuate the prevalence of Quartz peaks, which are distributed across 56% (SG-160) and 98% (SG-40).

Nevertheless, the analysis of carbonate minerals (calcite, dolomite, magnesium, and Ankerite) discloses substantial peaks mainly in the initial and middle sections of the core, particularly in SG-80, SG-100, SG-120, SG-140, and SG-160. Furthermore, there is an evident dominance of X-ray diffraction peaks corresponding to evaporite minerals (gypsum and halite) in SG-40 and SG-180. Conversely, minerals such as

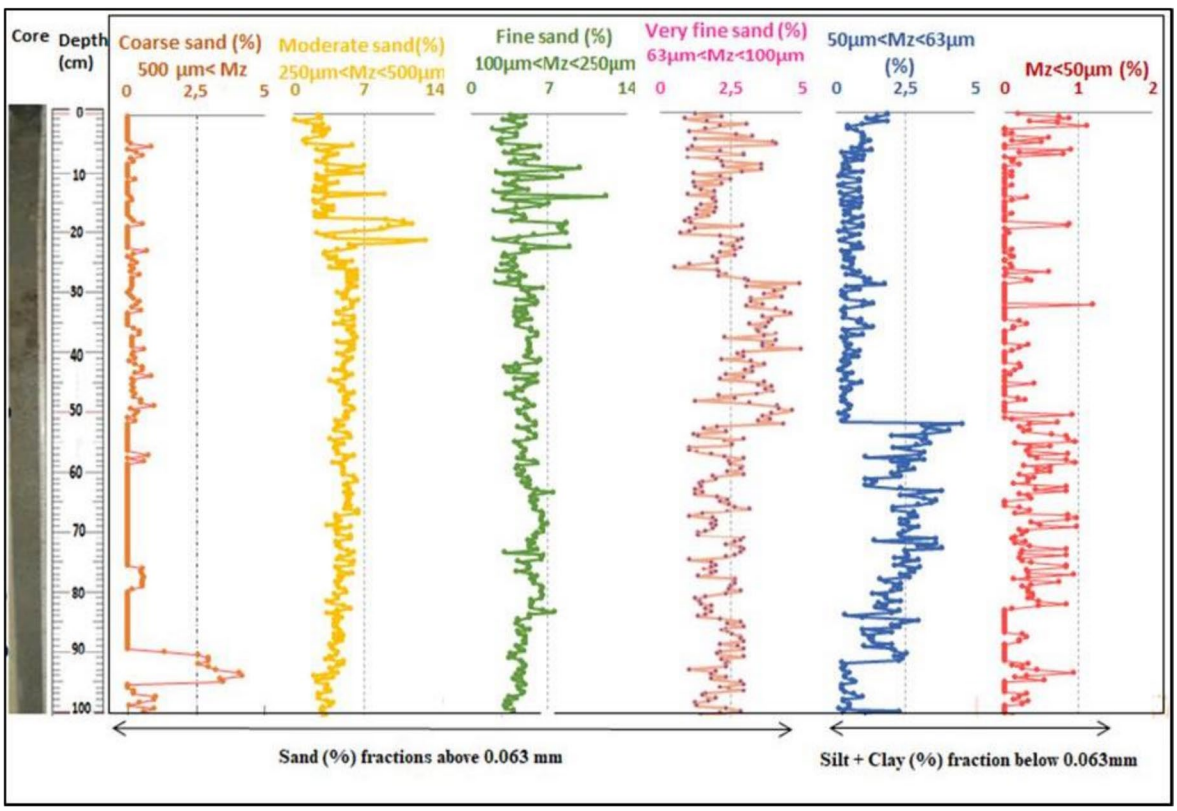

Fig. 2 Grain size evolution (lower fraction percentage of 0.063 mm and upper fraction percentage of 0.063 mm) of the Sebkha El-Guettiate

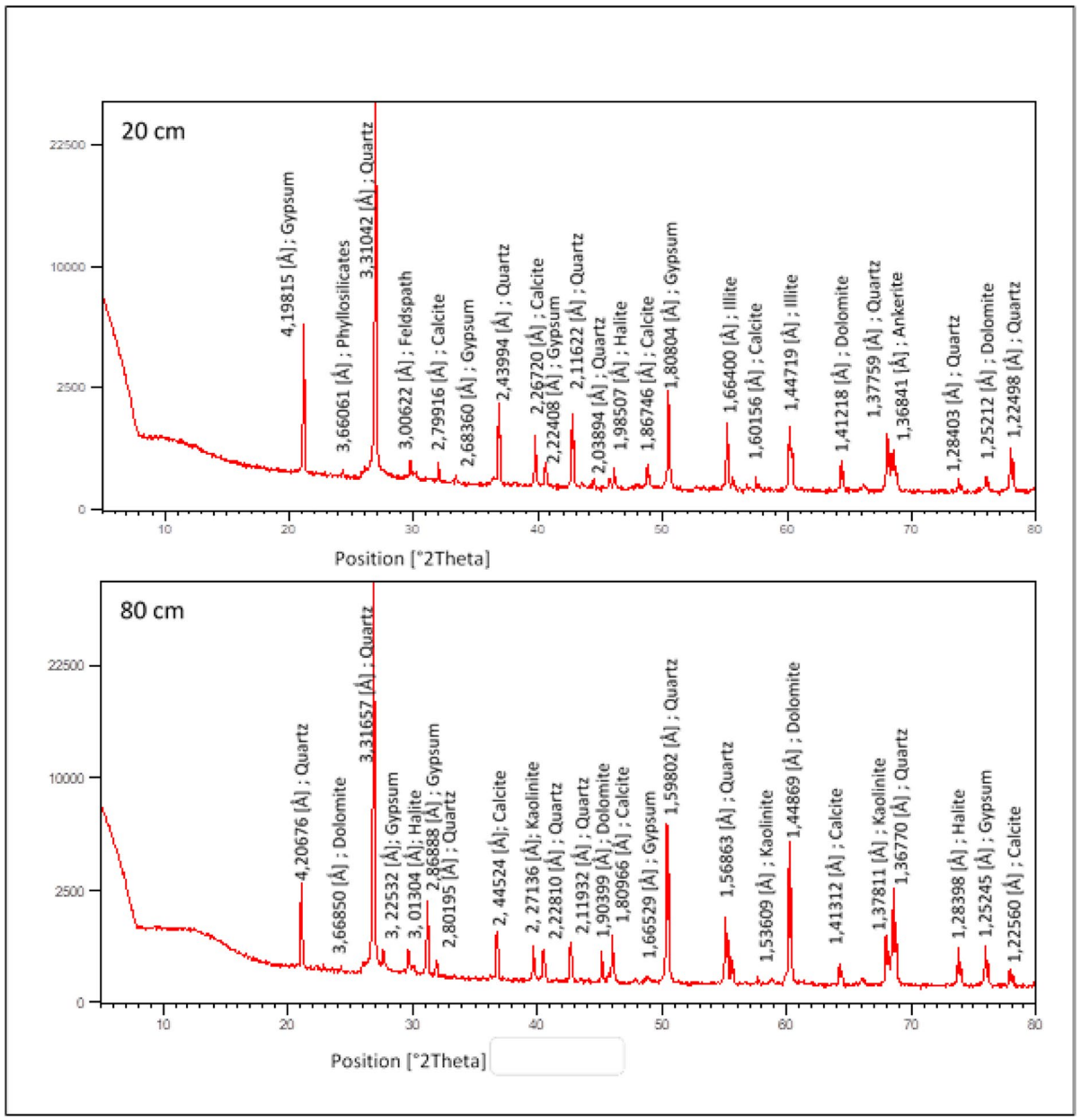

Fig. 3 X-ray diffractograms of the whole rock (samples SG-40 and SG-160) of the Sebkha

illite, phyllosilicates, and feldspar exhibit relatively lower abundance within this Sebkha core.

Scanning electron microscope

After determining the mineralogical compositions, the Sebkha sediments were identically examined using scanning electron microscopy images with energy-dispersive X-ray. Following results, SEM/EDX images generally show representations of quartz minerals (Fig. 4a), which were granted in all samples. In addition, types of clay were observed like illite. A pyrite mineral (FeS2) in automorphic form was also observed (sample SG-150) (Fig. 4f). However, carbonate minerals (calcite and dolomite) exist in almost all samples in the form of rhombohedral crystals

Table 1 Percentages of the mineralogical compositions of the El-Guettiate Sebkha core (Qz: quartz; Felds: feldspar; Ca: calcite; Ank: ankerite; D: dolomite; Gyp: gypsum; H: halite; Ka: kaolinite; I: illite)

Samples	Qz (%)	Felds (%)	Ca (%)	Ank (%)	D (%)	Gyp (%)	H (%)	Ka (%)	I (%)
SG-20	87	0	8	0	1	3	1	0	0
SG-40	98	0.5	1.5	0	0	0	0	0	0
SG-60	79	0	2	0	6	9	2.5	1	0
SG-80	88	2	0	3	4	0	2	0	1
SG-100	69	1	14	2	7	3	1	2	1
SG-120	90	0	1	1	3	1	3	1	0
SG-140	83	0	4	1	2	1	6	1	2
SG-160	56	3	11	1	3	14	9	1	2
SG-180	75	0	7	0	8	6	2.5	0	1.5
SG-200	86	0	2	0	5	4	1	1	0

(Fig. 4a,e). However, in evaporite minerals (gypsum and halite), halite can surround quartz crystals, which is also represented in almost all samples in cubic crystal form (Fig. 4c). While gypsum is found in the samples (SG-100 to SG-200), it is shown as white lamellae crystals (Fig. 4d).

The most common quartz grains are subrounded with the microtextural characteristics of aeolian grains: fresh curved cracks and percussion shapes (Ahmady-Birgani et al., 2023). Conchoidal fractures have sharp edges. The grains in this sample recorded a complex sedimentary history with alternating aeolian and aqueous environments (Zaîbi et al., 2011).

The oval mineral in Fig. 4b is a quartz primary mineral, which has been rounded and banded by carbonate; similar results are found by Lakhdar et al. (2006) in Sebkha Boujemmel (SE Tunisia), in Sebkha Mhabeul (SE Tunisia) by Gammoudi et al., (2021), and in Lake Urmia in Iran by Ahmady-Birgani et al. (2023). This shape shows that the ooid cortex is formed by superimposed carbonate crystals that may correspond to dissolution traces and microbial activity (Martín et al., 2020; Shen et al., 2022) and seem to be formed in a subtidal environment under moderated energy reflecting the fluctuating climatic conditions.

Kaolinite is a clay mineral, which probably has an inherited and detrital origin. The kaolinite amounts vary between 0 and 1%. Generally, it occurs in hot and humid intertropical regions in the oxidative environment (Molén, 2024), and it is considered as the alteration product of feldspars or illites (Gallela, 2010; Gammoudi et al., 2021). In fact, the coarser particles of clay aggregates in Fig. 4f have most probably aggregated in saline conditions; the same phenomena were registered in Korba lagoon (NE Tunisia) by Bouden and Chaabani (2004)and in Bizerte lagoon (north of Tunisia) by Srarfi et al., (2010).

The infrared spectrometer

Infrared spectrometry (IRTF) is an additional analytical technique employed in laboratories alongside chemical and mineralogical analyses. This method facilitates the examination of various aspects, including the chemical composition of vibrating ions, molecular group vibration patterns, and the identification of absorption bands' intensity and position, aiding in the interpretation of functional groups (Trabelsi, 2017). Typically, the wave number in such studies ranges from 4000 to 400 cm^{-1}. The FTIR (Fourier-transform infrared) results of the SG core samples (SG-20, SG-40, SG-60, SG-80, SG-100, SG-120, SG-140, SG-160, SG-180, and SG-200) are presented in Fig. 5.

Within these results, several distinct bands can be observed in succession.

- Notably, small and delicate absorption bands spanning 3226–3533 cm^{-1} and 3620–3712 cm^{-1} are prevalent across nearly all samples. These bands correspond to elongation vibrations of the OH groups of adsorbed water (Felhi, 2010).
- Existing research (Madéjova and Komadel, 2001; Madejova et al., 2002; Viscarra Rossel et al., 2006; Janik March–April, 2007; Truche, 2010) suggests that bands at 3500 cm^{-1}, 3575 cm^{-1}, 3620 cm^{-1}, 3694 cm^{-1}, and 3700 cm^{-1} can be attributed to the elongation

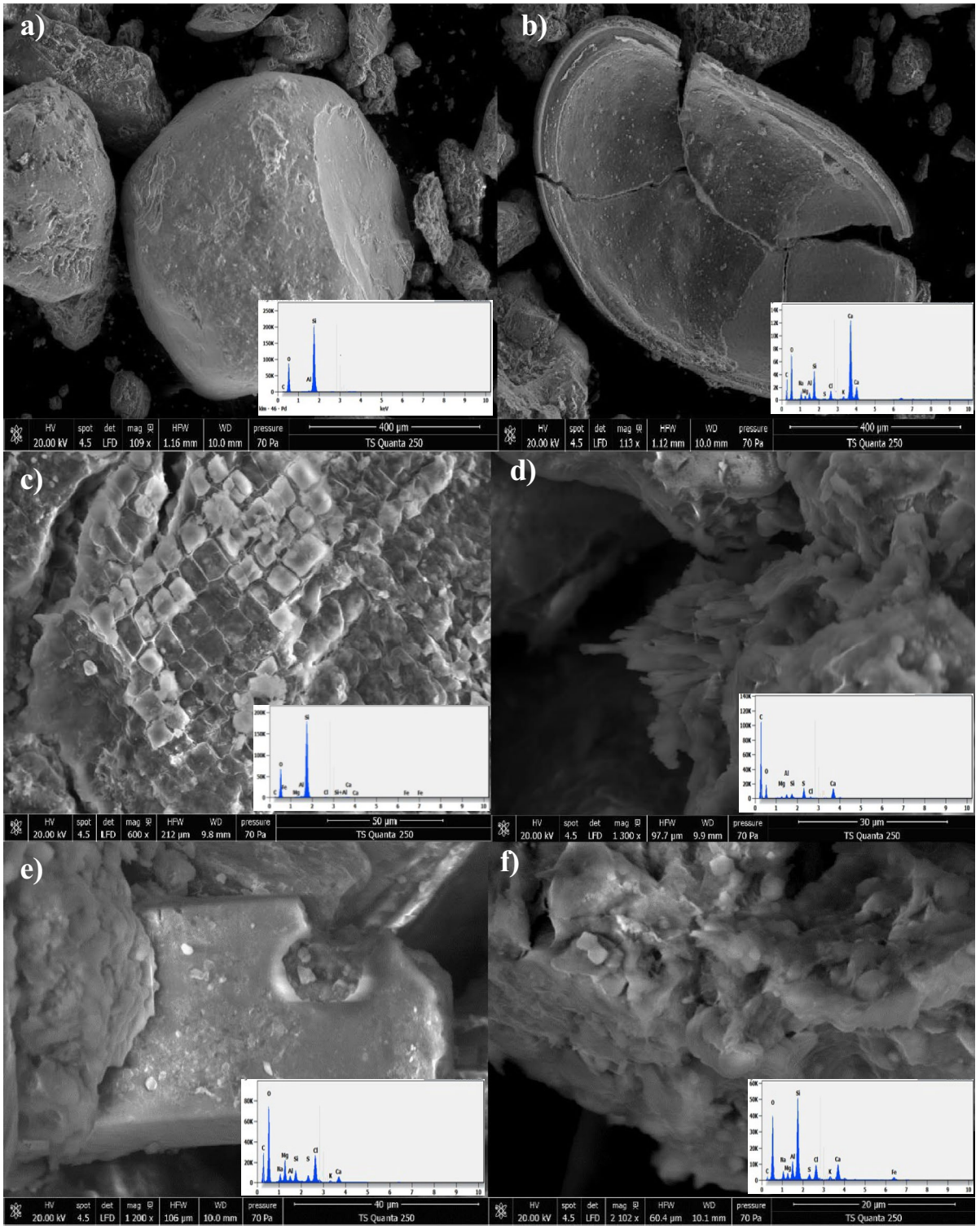

Fig. 4 Scanning electron microscope (SEM/EDX) images of sediment samples from the El-Guettiate Sebkha: (**a**) quartz, (**b**) calcite, (**c**) halite, (**d**) gypsum, (**e**) dolomite, and (**f**) clay minerals

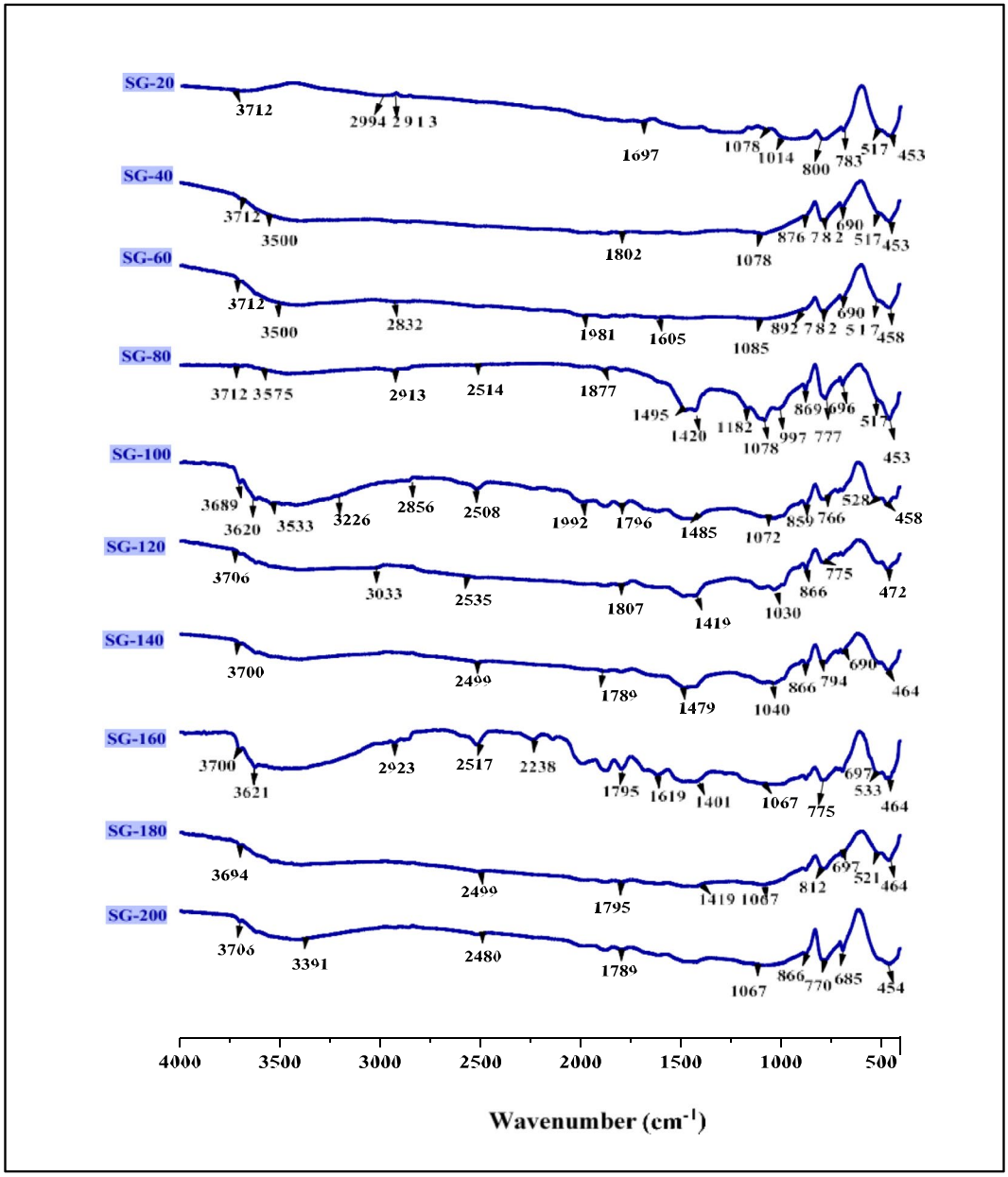

Fig. 5 Infrared spectra of Holocene sediments of the Sebkha El-Guettiate along the SG core

of the OH band in kaolinite. The absorption band at 3620 cm^{-1} is distinctive for kaolinite, setting it apart from illite and smectite (Truche, 2010).

- Additionally, the 3500 cm^{-1} band (observed in SG-40 and SG-60) is relevant to OH group vibrations in water molecules and OH deformation vibrations in kaolinite and gypsum (Yusuf, 2023).
- A minor peak absorption band, visible within the range of 2300–2500 cm^{-1} (SG-160, SG-180, and SG-200), indicates the vibration of the CO molecule in the presence of calcite (Truche, 2010). Additionally, a low-intensity wavenumber range spanning 2830–2950 cm^{-1} is observed in the SG-60, SG-80, and SG-160 samples, and these are associated with aliphatic CH3-CH2 groups

(Lakhdar, 2009; Kanbar et al. 2021). According to Sivakumar et al., (2012), this band signifies the vibration of the OH band in organic carbon.

- A distinctive band at 1870–1992 cm^{-1} is indicative of the stretching vibrations of Si–OH groups, pointing to the presence of quartz (Sivakumar et al., 2012).
- An intense band ranging from 1420 to 1795 cm^{-1}, prominent in the SG-80, SG-100, SG-120, SG-140, SG-160, SG-180, and SG-200 samples, signifies group elongation vibrations attributed to the presence of carbonates (Saikia et al., 2003; Sivakumar et al., 2012).
- A flattened and moderately noticeable absorption band around 1015–1120 cm^{-1} is evident in all samples and is linked to Si–O bands in kaolinite (Kanbar et al., 2021; Saikia et al., 2003; Sivakumar et al., 2012). Fine absorption band ranging from 990 to 1080 cm^{-1} corresponds to the vibration of the Si–O group in silicates (Kanbar et al., 2021; Trabelsi, 2017).
- A band situated at 850–880 cm^{-1} displays Al–OH deformation vibration in the presence of calcite (Saikia et al., 2003).
- An evident absorption band in all samples, found within the range of 770–794 cm^{-1}, is characteristic of the valence vibrations associated with Si–O band stretching in quartz and silicates (Saikia et al., 2003; Sivakumar et al., 2012).
- A band located at 517–533 cm^{-1} corresponds to the deformation vibrations of the Al–O–Si group in the presence of kaolinite (Saikia et al., 2003; Sivakumar et al., 2012; Trabelsi, 2017).
- A consistent band at 453–464 cm^{-1} is observed across all samples and is attributed to Si–O bands in feldspars (Sivakumar et al., 2012).

In conclusion, the FTIR technique proves to be a fundamental method for the mineral analysis of quartz, kaolinite, calcite, feldspar, and organic carbon.

Geochemical study

Bernard calcimetry

The variation in the calcium carbonate (CaCO3) contents of the samples analyzed along the core studied varies between 11 and 26%, allowing for modification that the CaCO3 contents are low and classified as little limestone. This classification of the calcium carbonate contents of the Sebkha El-Guettiate is probably due to the rainfall of calcite and/or dolomite. Indeed, the high value of $CaCO_3$ corresponds to a depth of 60–90 cm at the core. The results of the calcimetric methods will be testified later by X-ray fluorescence spectrometry by assembling the results with those of the mineralogical study Table 2.

X-ray fluorescence spectrometry

The results of the X-ray fluorescence technique are represented in the curves which are specific to the evolution of the percentages of the chemical elements (SiO2, CaO, MgO, Na2, O, Al2 O3, Fe2O3, MnO, TiO2, SO3, and K2O) as a function of core depth (Fig. 6). These results show that the variations of the contents of the elements CaO, MgO, Na2O, Al2O3, Fe2O3, MnO, TiO2, SO3, and K_2O are absolutely comparable to the core depth, which also become in the opposite direction corresponding to the SiO_2. According to geochemical and mineralogical analysis, this study is very rich in silica variation: between 81.4% (SG-130) and 88.43% (SG-50), but the percentages of other elements [for Na_2O between 0.16% (SG-50) and 0.54% (SG-90) and for K_2O between 0.31% (SG-170) and 0.7% (SG-110)]; finally, the Fe2O3 levels vary between 0.14% (SG-50) and 0.61% (SG-90). CaO levels vary between 3.16% (SG-10) and 6.6% (SG-110); those in MgO vary between 0.22% (SG-30) and 0.54% (SG-90), and for Al_2O_3,

Table 2 Correlation matrix of organic matter parameters with core depth

Variables	S1	S2	T_{max}	COT	IH	Depth
S1	**1**					
S2	**0.755**	**1**				
T_{max}	**0.842**	**0.746**	**1**			
COT	**0.871**	**0.980**	**0.857**	**1**		
IH	0.254	**0.897**	**0.534**	**0.792**	**1**	
Depth	-0.350	-0.479	-0.613	-0.495	-0.410	**1**

they vary between 1.21% (SG-190) and 2.3% (SG-110) for the core Fig. 7.

Organo-geochemical study

For this part, Rock–Eval 6 is used based on the estimation of the total organic carbon content (TOC) of the sediments. The data presented in Table 3 shows the results of the following parameters: TOC, HI (hydrogen index), IO (oxygen index), T_{max} (maximum temperature), S1 (quantity of free hydrocarbon compounds), S2 (amount of potential hydrocarbon compounds), and S3 (oxygenated compounds). However, this technique admits the resolution of the parameters of the geochemical analysis (Lafargue et al., 1998). The maximum temperature values of the core samples vary between 355 °C (SG-120) and 440 °C (SG-100). Table 3 shows the values of the percentages of total organic carbon which vary between 0.1 and 0.32%; the values of S1 vary between 0.11 mg of HC/g of sediment (SG-140) and 0.22 mg of HC/g of sediment (SG-60); the values of S2 correspond to 0.16 mg of HC/g of sediment (SG-160) to 1.02 mg of HC/g of sediment (SG-1); S3 modifies only 0.48 mg of HC/g of sediment in the SG-20 sample to 1.38 mg of HC/g respectively in the SG-60 sample. The variations in the hydrogen indexes (HI) are characterized by a higher value for the SG-160 sample of 206 mg HC/g of TOC and 331 mg of HC/g of TOC for the SG-1 sample. The IH versus IO diagram (Fig. 8), leading to the elemental composition of a large number of samples without minerals (Disnar et al., 2013), shows that the majority of samples from the core of Sebkha El-Guettiate particularly decrease in IH as depth increases in the sediment core. It may correspond to the mineralization of organic matter and the continental origin of the organic stock.

Indeed, at Rock–Eval, the maximum temperature (T_{max}) is characterized by a slight variation from 355 to 440 °C, the highest peak being 440 °C for the SG-100 sample.

Statistical analysis of results (ACP)

We used the multivariate method of principal component analysis (PCA) to complete the factorial relations (F1 × F2) of the matrix of correlations between the parameters of the mineralogical compositions and the elements of the minerals and the parameters of organic matter of the carrot SG (Fig. 7).

The eigenvalues characterize that the first factorial plane, composed of the axes F1 and F2, explains

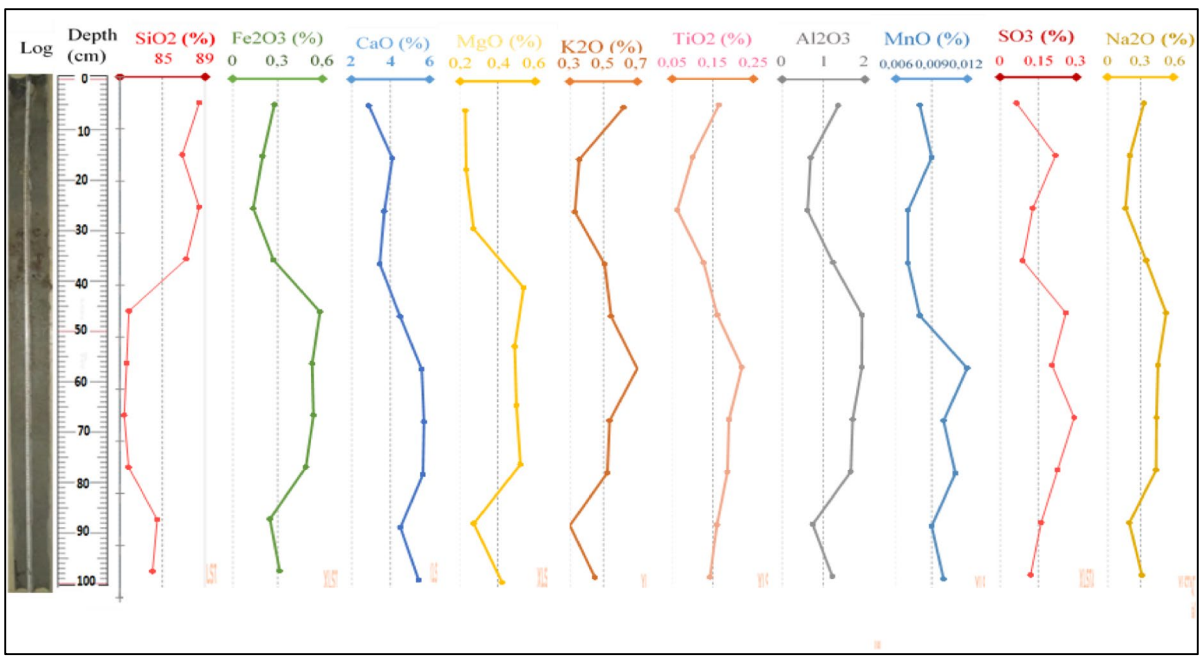

Fig. 6 Vertical variation of the chemical elements of the core samples studied

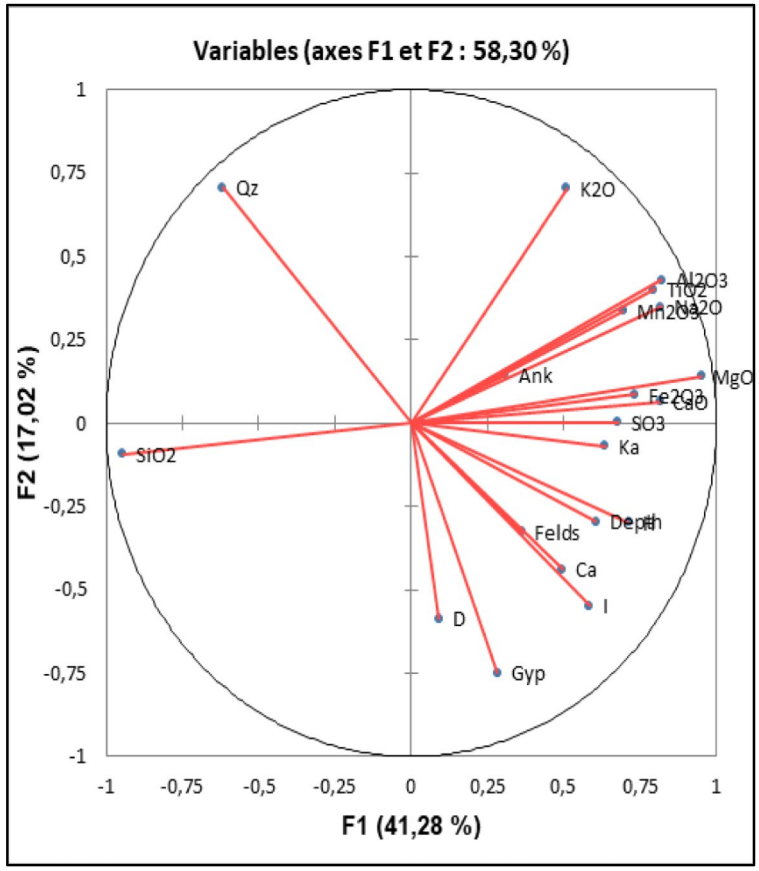

Fig. 7 Principal component analysis of mineralogical parameters (Qz: quartz; Felds: feldspar; Ca: calcite; Ank: ankerite; D: dolomite; Gyp: gypsum; H: halite; Ka: kaolinite; I: illite) and parameters of the mineral elements of the Sebkha El-Guettiate core

Table 3 Results of organic matter parameters and SG core depth by Rock–Eval technique 6

Depth (cm)	N° sample	Quantity (mg)	S1 (mg d'HC/g de roche)	S2 (mg/g)	T_{max} (°C)	S3 (mg d'HC/g de roche)	COT (%)	IH	IO
0,5	SG-1	74,3	0,21	1,02	430	1,14	0,32	331	320
10	SG-20	76	0,16	0,3	425	0,48	0,17	269	413
20	SG-40	63,8	0,23	0,46	429	0,69	0,31	243	332
30	SG-60	71	0,22	0,57	435	1,38	0,21	228	443
40	SG-80	67,5	0,19	0,61	420	1,17	0,26	239	416
50	SG-100	72,4	0,25	0,76	440	0,89	0,25	226	481
60	SG-120	78,9	0,18	0,37	355	0,96	0,13	212	898
70	SG-140	76,4	0,11	0,29	358	1,36	0,11	234	931
80	SG-160	72,3	0,13	0,16	360	1,24	0,14	206	754
90	SG-180	76,1	0,13	0,34	360	1,08	0,1	218	1011
100	SG-200	61,2	0,19	0,96	430	1,12	0,29	292	369

58.30% of the total inertia. Axis I formulates 41.28% of the core depth variance, which is positively correlated with quartz and calcium carbonate. Then, we explained a good positive correlation between CaO and MgO ($R^2 = 0.79$), between TiO2 and Al2O3 ($R^2 = 0.76$), between Na2O and Al2O3 ($R^2 = 0.98$), between Al2O3 and MgO ($R^2 = 0.88$), and between Al2O3 and K2O ($R^2 = 0.87$) (Table 3). The graphs

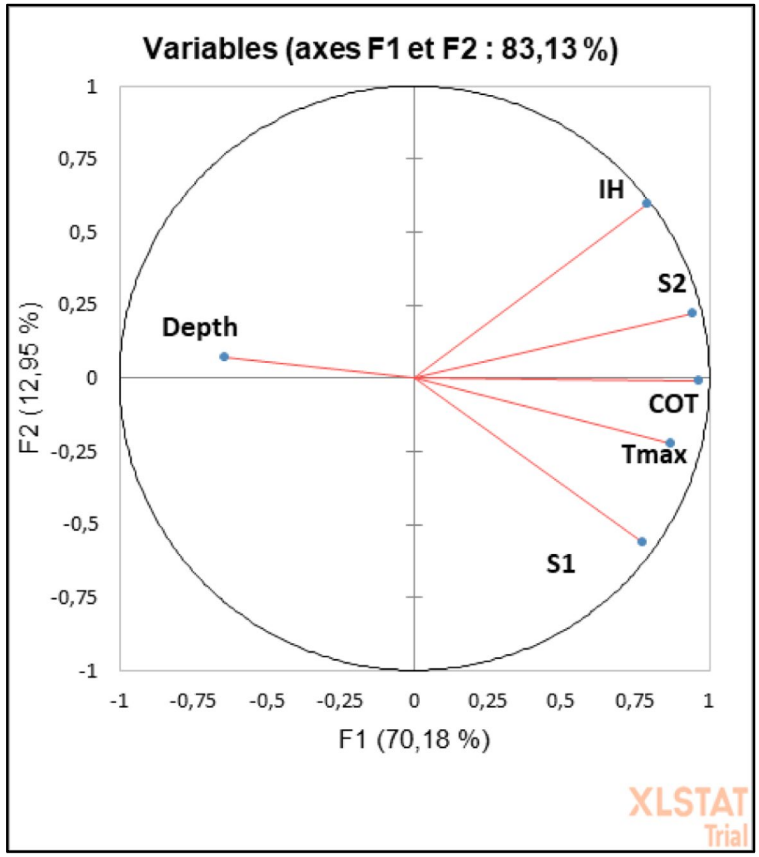

Fig. 8 Factorial plane of organic matter parameters with core depth

resulting from the factorial analysis make it possible to determine parameters of organic matter express 83.13% of the variance (Fig. 8 and Table 2), highlighting the design of homogeneous group statistics.

According to the factor (F1×F2), it has been shown a good positive correlation between S1 and S2 ($R^2=0.755$), between T_{max} and S1 ($R^2=0.842$), between COT and S1 ($R^2=0.871$), between T_{max} and S2 ($R^2=0.746$), between COT and S2 ($R^2=0.980$), between IH and S2 (R^2 352 = 0.861), between COT and T_{max} ($R^2=0.857$), and between IH and COT ($R^2=0.792$), but we observe a correlation negative all the parameters with the core length depth (Table 2).

The hydrogen index (IH) diagram as a function of the oxygen index (IO) (Fig. 8), providing information on the origin of the organic matter (Koegel-Knabner and Rumpel (2018), indicates all the samples of the core had heterogeneous organic matter with both marine and terrestrial origins. It is characterized by a variation of 355 to 440 °C of the maximum temperatures of peak 2. Organic matter (OM) is richer in humic matter which begins to mineralize to become lignified OM.

Discussion

Deposit sedimentology and the environment

The investigation of the sedimentary environment leads us to the conclusion that a significant portion of the sands within Sebkha El-Guettiate originates from a marine-like setting and common quartz grains are subrounded with characteristics of aeolian grains like fresh curved cracks and percussion shapes (Ahmady-Birgani et al., 2023).

Although multiple conchoidal fractures can also form in aeolian or aqueous environments, the impact of wind is more likely, as the high energy required to create such fractures in the water is not compatible with the characteristics of frequent precipitation and the abundance of euhedral

NaCl crystals (Battiau-Queney et al., 2023). On the other hand, strong onshore winds can generate a temporarily high level of wind energy, especially described by Ouaja et al., (2013) as responsible for Aeolian transport in golf of Gabes.

The predominant sedimentary makeup in the studied region consists of the sandy fraction, which is notably enriched in carbon. The surface of the Sebkha is notably abundant in the salt crust (composed of gypsum and halite), which indicates a relationship with the Mediterranean Sea, particularly during instances of Sebkha flooding. This communication is particularly prominent in this specific area. According to Chen and Hur (2015), the sedimentary layers contain organic matter that primarily comprises humic substances or organic residues complexed through less soluble chemical processes. However, within deposits, the presence of organic matter becomes significant for bacterial activity (Pacton et al., 2007). Within this Sebkha, the gypsum crystals are observed to break down into sandy and silty levels during the process of evaporation. As stated by Pomel et al., (2008), during rainy periods, the coexistence of a gypsum and organic matter layer, fostering the presence of bacteria, signifies an alternating pattern between dry and flood conditions.

Contribution of chemical elements and mineral source

The examination of Sebkha sediments involves the utilization of mineralogical composition, as well as FTIR, SEM/EDX, and XRD analyses. The outcomes of the mineralogical assessments of sediment samples are intricately tied to the distinctive nature of various mineral constituents within the overall rock structure, as outlined in Table 1. This investigation encompasses a range of minerals including dolomite, calcite, gypsum, quartz, illite, ankerite, halite, and feldspar.

The variations in the composition of non-clay minerals offer insights into the distinguishing features of the sediments. Notably, calcite is prevalent across the majority of core sediments, accounting for proportions that range from 1 to 14%. The distribution of these percentages suggests a potential origin through chemical precipitation, biochemical processes, or interactions involving organisms with limestone formations. Quartz exhibits notably high proportions relative to other minerals in all sampled sediments, ranging from 56 to 98%. As indicated by Gargouri (2011), surface sediments from the distant regions of Sebkha El-Guettiate and the mouths of wadis (wadi El-Guettiate, wadi Aouien, and wadi Bou Said) originate from the quaternary emergence of the Gabes golf course.

Furthermore, the occurrence of dolomite is relatively low, with percentages ranging from 1 to 8% along the core scales (Table 1). The origins of this mineral are attributed to either direct precipitation from seawater or certain marine substances such as algae and foraminifera (as cited in Arrim, 1996; Cappellen, 2003).

However, the presence of clay minerals, specifically the kaolinite fraction < 0.2 µm, constitutes a minor percentage ranging from 0 to 2% in certain sediment samples.

Upon analyzing the correlation matrix table, we observe several notable trends. Feldspar exhibits negative correlations with quartz ($R^2 = -0.57$). This could be attributed to the mineral's continental detritus origin (Chairi, 2004).

The carbonate levels within the core sediments reveal a prevalence of calcite in comparison to dolomite. First, it could be a result of the erosion of adjacent carbonate-rich land formations. Alternatively, it might stem from a chemical process involving the direct precipitation of CaCO3. Comparable findings have been reported in the Tunisian South East (as mentioned by Gargouri, 2011; Bouaziz et al., 2015; Lakhdar et al., 2021) and the Tunisian Sahel (Tagorti, 1990).

The mineralogical analysis results find support in the X-ray fluorescence spectrometer analyses performed on the same core samples, revealing a SiO_2 content ranging from 81.39 to 88.84%.

The geochemical composition results, characterized by generally low CaCO3 content, strongly suggest a chemical origin related to evaporation, indicating a humid climate. The carbonate contents might be a result of siliceous dissolution, accompanied by the accumulation of magnesium, which contributes to progressive dolomitization.

Geochemical analyses also reveal a negative correlation between CaO (from calcite) and SiO2 (from quartz) (Table 4). Sediments in the core displaying higher levels of Al2O3, SiO2, and CaO may be linked

to the dissolution of evaporites and the precipitation of clay minerals (Gallela, 2010), which is indicated by a positive correlation (Table 4). Interestingly, the vertical variations in hydroxides Na2O, Al2O3, CaO, K2O, TiO2, MgO, MnO, SO3, and Fe2O3 within the core sediments follow a parallel trend, while SiO2 levels exhibit an opposing pattern (Fig. 6). This progression suggests the presence of phyllosilicates (Bouden and Chaabani, 2004; Gammoudi et al., 2021).

The positive correlation ($R^2 = 0.79$) observed between MgO and CaO signifies the presence of dolomite, a mineral closely associated with feldspar (Warren, 2000). At an oceanic level, the constancy in Mg levels, combined with variations in seabed diffusion, leads to the replacement of Ca levels within seawater. Consequently, this mineralogical phenomenon contributes to the dominance of marine carbonate and evaporite precipitates.

Additionally, Table 4 reveals a significant positive correlation between Al2O3 and TiO2 ($R^2 = 0.81$). The element Ti is especially present within phyllosilicates as detrital minerals (Dabard, 1990; Condie et al., 1992; as referenced in Gammoudi et al., 2021).

Figure 6 demonstrates robust positive correlations among various chemical elements in core sediments, including K2O/Al2O3, K2O/Fe2O3, TiO2/Al2O3, and Al2O3/SiO2. These elements are generally attributed to illite, feldspars, and kaolinite. The TiO2/Al2O3 binary diagram, in particular, displays a positive correlation ($R^2 = 0.67$) for the core samples. The correlation between K2O/Al2O3 also exhibits a strong positive trend ($R^2 = 0.76$) within core sediments, highlighting the abundance of aluminous components. Similarly, the correlation between K_2O/Fe_2O_3 and Al_2O_3/SiO_2 demonstrates substantial positive correlations ($R^2 = 0.57$ and $R^2 = 0.59$ respectively) within core sediments. As indicated by Gallela (2010), these associations point to the presence of various minerals, involving iron clay minerals, oxides, and iron hydroxides (Srarfi et al., 2019). The relationship between K2O and Fe2O3 is primarily influenced by the presence of illite and kaolinite alterations, as well as the prevalence of feldspars (Bouden and Chaabani, 2004; Gallela, 2010).

Notably, all samples exhibit richness in Al_2O_3 and SiO_2, indicative of the presence of clays. Generally, the larger quartz grains observed along the core represent the dominant Aeolian sediment constituents. The clays of the Sebkha are inherited, and therefore, their composition reflects the procession of clay minerals of the watershed soils. They are characterized by an enrichment of kaolinite and illite. The study of the clays shows the similarity of the procession in the upper levels with that of the sedimentary column, which underlines the constancy of the terrigenous feeding. The same results are found in Korba lagoon in the NE of Tunisia (Bouden and Chaabani, 2009).

Certainly, the investigation into organic matter involves determining the total organic carbon (TOC) content of core samples, which exhibits a range from 0.1 to 0.32%. These values are lower than COT registered in other similar systems in Tunisia (Tunis lagoon from 1 up to 1.69%, Korba from 0.48 up to 5.21% (Bouden and Chaabani, 2004), Moknine from 0.3 to 1.7% (Chairi et al., 2010), Sidi El Hani and Mejerda mouth from 1.13 to 2.63% (Triki et al., 2022)). This is in relation to the silty and sandy sediment nature and core location in a sea pass. The low values are due to OM mineralization due to environmental conditions, along with T_{max} values below 440 °C (Table 3). T_{max} values above 300 °C indicate that the organic matter in the sebkhet El-Guettiate is not residual and highly altered. The origin of OM under these conditions is difficult to determine (Triki et al., 2022), but Rock–Eval analysis suggests that it is richer in lignin in the subsurface and humic compounds. Likewise, the T_{max} suggests that much of the OM in the Sebkha may be humic or fulvic acids since temperatures are between 300 and 400 °C (Disnar et al., 2013). Land-based OM in sediments contains abundant humic compounds to which lignin can also adhere. The high content of S3 attest to the presence of terrigenous plants OM (Chairi, 2005) source of the fragments of lignin. These humic compounds are a likely source of refractory carbon for the anaerobic bacteria metabolism, especially in the presence of Mn oxides (Table 3) (Triki et al., 2022).

Nevertheless, some general trends, especially low TOC and HI values (206–331), are related to intense oxidation for the permanently emerged core (Chairi et al., 2010). The IH versus IO diagram (Fig. 8), leading to the elemental composition of a large number of samples without minerals (Disnar et al., 2013), shows that the majority of samples from the core of Sebkha El-Guettiate particularly decrease in IH as depth increases in the sediment core. According to the two diagrams (Fig. 9), there are two separate stocks of OM, probably originating from different sources.

Table 4 Correlation matrix of mineralogical compositions and mineral element parameters of Sebkha El-Guettiate core (Qz: quartz; Felds: feldspar; Ca: calcite; Ank: ankerite; D: dolomite; Gyp: gypsum; H: halite; Ka: kaolinite; I: illite)

Variables	Qz	Felds	Ca	Ank	D	Gyp	H	Ka	I	Depth	Fe2O3	MgO	SiO2	CaO	K2O	TiO2	SO3	Al2O3	Mn2O3	Na2O
Qz	**1**																			
Felds	−0.57	**1**																		
Ca	−0.77	0.33	**1**																	
Ank	−0.16	**0.62**	0.08	**1**																
D	−0.47	−0.05	0.28	0.11	**1**															
Gyp	−0.81	0.43	0.44	−0.25	0.31	**1**														
H	−0.66	**0.53**	0.26	0.14	−0.08	**0.61**	**1**													
Ka	−0.49	0.07	0.43	0.22	0.36	0.23	0.23	**1**												
I	−0.69	0.48	0.43	0.34	0.24	0.41	**0.77**	0.18	**1**											
Depth	−0.42	0.07	0.11	−0.03	0.47	0.31	0.43	0.29	0.44	**1**										
Fe2O3	−0.32	0.06	0.20	−0.14	−0.07	0.22	**0.66**	0.17	0.46	**0.52**	**1**									
MgO	−0.50	0.26	0.45	0.33	0.08	0.14	**0.53**	**0.78**	0.39	**0.53**	**0.57**	**1**								
SiO2	0.44	−0.17	−0.37	−0.25	−0.14	−0.09	−0.54	−0.64	−0.48	−0.67	−0.71	−0.92	**1**							
CaO	−0.31	0.08	0.06	−0.01	0.04	0.19	0.58	**0.51**	0.37	**0.78**	**0.75**	**0.79**	−0.89	**1**						
K2O	0.02	0.11	0.14	0.40	−0.38	−0.25	0.18	0.28	−0.14	−0.10	0.28	**0.57**	−0.40	0.29	**1**					
TiO2	−0.22	0.08	0.31	0.20	−0.13	−0.07	0.45	0.22	0.28	0.43	**0.76**	**0.72**	−0.76	**0.59**	**0.73**	**1**				
SO3	−0.30	0.10	0.32	0.13	−0.05	0.06	0.43	**0.56**	0.50	0.27	**0.61**	**0.66**	−0.77	**0.67**	0.09	0.38	**1**			
Al2O3	−0.30	0.25	0.41	**0.51**	−0.11	−0.98	0.38	**0.60**	0.23	0.20	0.44	**0.88**	−0.74	0.49	**0.87**	**0.81**	0.45	**1**		
Mn2O3	−0.11	0.02	−0.01	−0.18	−0.25	0.18	0.49	0.22	0.09	**0.56**	**0.83**	**0.63**	−0.74	**0.85**	0.41	**0.74**	0.48	0.49	**1**	
Na2O	−0.35	0.35	0.46	**0.61**	−0.07	−0.13	0.37	**0.62**	0.30	0.20	0.36	**0.88**	−0.74	0.47	**0.85**	**0.74**	0.49	**0.98**	0.41	**1**

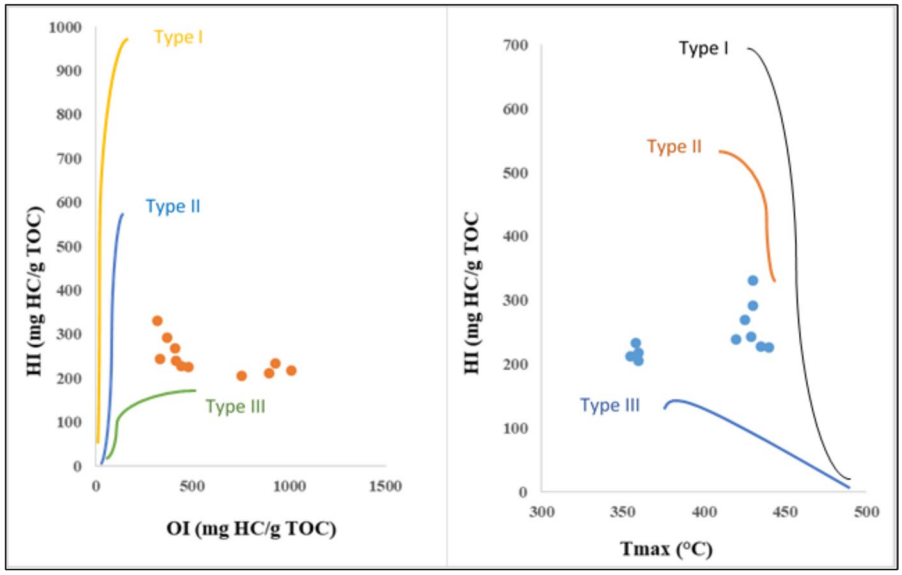

Fig. 9 Position of samples in the IH/OI and IH/T_{max} diagram and MO types based on Espitalié et al., (1977)

Table 5 Comparative geochemical, grain size, and mineralogy of sediments in Sebkha El-Guettiate

	Major elements	Minerals	Grain size	COT	Author
This study – Sebkha El-Guettiate	Ca. 2 and 6%, Mg. 0 and 4%, Na. 3 and 6%, K. 0 and 3%	Cal. 0 and 14%, Gyp. 0 and 14%, Dol. 0 and 8%, Hal. 0 and 9%, Qz. 56 and 98%	Silt /Sand	0.1 and 0.32%	Present study
Sebkha Mhabeul South – Eastern Tunisia	Ca. 0 and 8%, Mg. 4 and 7%, Na. 15 and 55%, K. 0 and 2%	Cal. 1 and 20.6%, Gyp. 1 and 18.1%, Dol. 1 and 8.4%, Hal. 2 and 14%, Qz. 44 and 92%	Clay sand	0.1 and 0.43%	Gammoudi et al., (2021)
Sebkha khor Al-Adaid Qatar	Ca. 6 and 12%, Mg. 5 and 20%, Na. 15 and 28%, K. 4 and 7%	Cal. 1 and 6%, Gyp. 5 and 25%, Dol. 2 and 8%, Hal. 1 and 12%, Qz. 0 and 8%	Clay sand	ND	Al Disi et al., (2023)
Sebkha Kadim Alaa'ab Iraq	Ca. 8 and 15%, Mg. 0 and 1%, Na. 19 and 28%, K. 1 and 2%	Cal. 1.8 and 13%, Gyp. 3 and 19.1%, Dol. 0 and 5%, Hal. 50 and 80.2%, Qz. 1 and 11%	Clay Sand	ND	Mohammad and Awadh (2023)
Salton Sea – California	ND	Cal. 4 and 19%, Gyp. 1 and 19%, Dol. 3 and 8%, Hal. 18 and 54%, Qz. 3 and 40%	Clay sand	ND	Buck et al., (2011)

ND, not determined by the author

The infrared spectra obtained from the core sediments of El-Guettiate Sebkha (Fig. 5) display prominent OH deformation vibration absorption bands, CO bands, and aliphatic structures CH3-CH2 indicating IO oxygenated compounds (C-H, COOH…).

Chairi, in 2018, was found in Moknine Sebkha (a very similar environment to Sebkha El-Guettiate) at the edge of the Sebkha, where the facies is sandy or silty, the origin of the organic matter is mixed. The OM is continental in early digenesis in relation to the arid climate about 150 years ago. This outcome aligns with the mineralogical components observed.

We can compare the geochemical, granulometric, and mineralogical results of the sediments of the

Sebkha El-Guettiate during the Holocene with other studies: Sebkha Mhabeul South – Eastern Tunisia, Sebkha khor Al-Adaid Qatar, Sebkha Kadim Alaa'ab Iraq, and Salton Sea – California (Table 5). We found that Tunisian Sebkhas had a similar composition of major elements as well as minerals. They denote similar climatic and sedimentation environments. Therefore, some singular characteristics should be mentioned. In Sebkha Kadim Alaa'ab Iraq, high evaporation rates are observed as water evaporates from shallow basins, leading to salt crystallization (Mohammad & Awadh, 2023). Microbial mats are present on the surface of Sebkha khor Al-Adaid Qatar, despite the fact that evaporitic minerals frequently accumulate below the surface. High salinity is demonstrated by high evaporation rates (Al Disi et al., 2023). In the Salton Sea – California, salt minerals with acicular or prismatic properties are more likely to be disruptive, increasing salt uplift (Buck et al., 2011). Sebkha El-Guettiate has lower concentrations of evaporitic minerals and salts (Na, Ca, Mg, and K), which may indicate less favorable conditions for high evaporation, probably due to the continuous communication with the sea. The clay components are greater than those found in Sebkha El-Guettiate. In fact, the core is taken in the middle of the depression in low-energy sedimentation. El-Guettiate's sandy core is influenced by Mediterranean Sea dynamism.

Conclusion

The El-Guettiate Sebkha, situated in southeastern Tunisia, is recognized for its deposition of sandy and loamy fractions. An assessment of mineralogical parameters reveals that non-clay minerals encompass evaporites (halite and gypsum), silicates (quartz and feldspar), and carbonates (calcite, dolomite, magnesium, and ankerite). Additionally, clay minerals, predominantly kaolinite and illite, are present. Remarkably high quartz content percentages, ranging from 56 to 98%, are observed with an obvious Aeolian contribution.

The compositional variations of non-clay minerals allow for the identification of exposed calcite, which is abundant in the majority of core sediments, with proportions ranging from 1 to 14%. Calcite's presence suggests a chemical origin via precipitation and/or biochemical processes involving the interaction of organisms with limestone formations. Generally, fluctuations in carbonate content (CaCO3) indicate that elevated CaCO3 levels correspond to dry climates that favor evaporite accumulation. Conversely, lower contents point toward carbonate dissolution in humid climates.

Geochemical analyses highlight the dominance of the Si element, primarily sourced from quartz. The major elements (Mg, Ca, Na, Cl, and K) predominantly stem from minerals like dolomite, halite, gypsum, phyllosilicates, and potassium feldspar. Infrared spectrometry corroborates the mineralogical findings, confirming the presence of both aliphatic (CH_2, CH_3) and aromatic (C=O) structures. Investigating sedimentary organic matter offers insights into organic components resulting from aquatic production. El-Guettiate core has relatively low TOC values (ca. 0.1–0.32%). No significant difference is apparent in terms of OM content among the depth. Such features are thought to reproduce permanent emersion and dryness of the Sebkha borders, which results in extensive oxidative degradation of the OM.

This underscores the diverse origins contributing to Sebkha sediment formation, often influenced by saline systems.

However, this study remains preliminary, which needs to be followed by further study and future research that will provide finer microscopic analyses and include a more detailed assessment of sand morphoscopy to complement a more integrated micromorphological assessment and more involved in pedo-sedimentary events of the study area.

Acknowledgements In this work, Dr. Ahmed Hichem Hamzaoui, Bachir Slimi, and Ramzi Ben Massoud are acknowledged for their help and assistance in the geochemical field and mineralogical analysis at the Borj Cedria Technopole Center and Mr. Mohamed Lassoued, director of CRDA Sfax, Dr. Mabrouk Boughdiri, chef department de faculty of sciences of Bizerte University of Carthage Tunis, and Dr. Elhoucine Essefi for his contribution to the missions sampling.

Author contribution The authors significantly contributed to preparing, writing, and revising the manuscript. Najia Bouabid contributed to data interpretation and wrote the major manuscript, sampled, data collection and analyses. Feyda Srarfi contributed to writing and revising the manuscript. Hayet Mnasri and Mohamed Ali TAGORTI revised the manuscript. All authors read and approved the final manuscript.

Data availability The datasets used and analyzed during the current study are available from the authors upon reasonable request.

Declarations

Competing interests The authors declare no competing interests.

References

Ahmady-Birgani, H., Ravan, P., Yao, Z., & Afrasinei, G. M. (2023). Understanding saline lake sand dunes dynamics: Coupling remote sensing techniques and field studies. *CATENA, 232*, 107424.

Al-Hurban, A., Albanai, J. A., & Elrawy, M. (2023). Comparison study on sedimentomorphological characteristics using integrated geo-techniques: A case study of two representative areas in Kuwait. *Journal of Geographic Information System, 15*(1), 140–173.

Al Disi, Z. A., Naja, K., Rajendran, S., Elsayed, H., Strakhov, I., Al-Kuwari, H. A. S., & Al-Khayat, J. A. A. (2023). Variability of blue carbon storage in arid evaporitic environment of two coastal Sabkhas or mudflats. *Scientific Reports, 13*(1), 12723.

Armstrong, E., Tallavaara, M., Hopcroft, P. O., & Valdes, P. J. (2023). North African humid periods over the past 800,000 years. *Nature Communications, 14*(1), 5549.

Arnaud, F., Révillon, S., Debret, M., Revel, M., Chapron, E., Jacob, J., Giguet-Covex, C., Poulenard, J., & Magny, M. (2012). Lake Bourget regional erosion patterns reconstruction reveals Holocene NW European Alps soil evolution and paleohydrology. *Quat. Sci. Rev., 51*, 81–92.

Battiau-Queney, Y., Ventalon, S., Abraham, R., Sipka, V., Cohen, O., & Marin, D. (2023). Bedforms and sedimentary features related to water-depth variations in a sandy tidal-flat environment. *Journal of Coastal Research, 40*(1), 80–103.

Benito, G., Macklin, M. G., Zielhofer, Z., Jones, A. F., & Machado, M. J. (2015). Holocene flooding and climate change in the Mediterranean. *CATENA, 130*, 13–33.

Bedair, H., Alghariani, MS, Omar, E., Anibaba, QA, Remon, M., Bornman, C., ... et Alzain, HM (2023). Statut de réchauffement *climatique sur le continent africain : Sources, défis, politiques et orientation future. Revue Internationale de Recherche Environnementale, 17*(3), 45.

Bond, G., Kromer, B., Beer, J., Muscheler, R., Evans, M. N., Showers, W., Hoffmann, S., Lotti-Bond, R., Hajdas, I., & Bonani, G. (2001). Persistent solar influence on North Atlantic climate during the Holocene. *Science, 294*, 2130–2136.

Bouaziz, A., El Asmi, A. M., Skanji, A., & El Asmi, K. (2015). A new borehole temperature adjustment in the Jeffara Basin (southeast Tunisia): Inferred source rock maturation and hydrocarbon generation via one-dimensional modeling. *AAPG Bulletin, 99*(9), 1649–1669.

Bouden, S., & Chaabani, F. (2004). Geochemical characterization of lagoonal surface sediments: Case of the Korba Lagoon (Cap Bon, North East of Tunisia). *Geo-Eco-Trop, 28*(1), 15–26.

Bouden, S. and Chaabani, F. (2009) Dynamique sédimentaire de la lagune de Korba (Nord-Est de la Tunisie). https://doi.org/10.4000/quaternaire.5152

Buck, B. J., King, J., & Etyemezian, V. (2011). Effects of salt mineralogy on dust emissions, Salton Sea, California. *Soil Science Society of America Journal, 75*(5), 1971–1985.

Chairi, R. (2004). *Etude du remplissage sédimentaire récente et de la matière organique associée, dans la sebkha de Moknine*. Univ, Tunis El Manar, Faculty of Sciences of Tunis.

Chairi, R. (2005). Etude du remplissage sedimentaire d'un systeme hypersalin de la Tunisie orientale au cours du Quaternaire recent: La Sebkha de Moknine. *Quaternaire, 16*, 107e117.

Chairi, H., Fernández-Diaz, C., Navas, J. I., Manchado, M., Rebordinos, L., & Blasco, J. (2010). In vivo genotoxicity and stress defences in three flatfish species exposed to CuSO4. *Ecotoxicology and Environmental Safety, 73*(6), 1279–1285.

Chen, M., & Hur, J. (2015). Pre-treatments, characteristics, and biogeochemical dynamics of dissolved organic matter in sediments: A review. *Water Research, 79*, 10–25.

Condie, C. K., Noll, P. D., & Conway, C. M. (1992). Geochemical and detrital mode evidence for two sources of Early Proterozoic sedimentary rocks from the Tonto Basin Super group, central Arizona. *Sedimentary Geology, 77*, 51–76.

Dabard, M. P. (1990). Lower Brioverian formations (Upper Proterozoic) of the Armorican Massif (France): Geodynamic evolution of source areas revealed by sandstone petrography and geochemistry. *Sedimentary Geology, 69*, 45–58. https://doi.org/10.1016/0037-0738(90)90100-8

Disnar, J. R., Guillet, B., Kéravis, D., Giovanni, C. G., & Sebag, D. (2013). Soil organic matter (SOM) characterization by Rock-Eval pyrolysis: Scope and limitations. *Organic Geochemistry, 34*, 327–343. https://doi.org/10.1016/S0146-6380(02)00239-5

El Arrim A (1996) Etude d'impact de la dynamique sédimentaire et des aménagements sur la stabilité du littoral du Golfe de Tunis. Diplôme de Doctorat de Spécialité en Géologie. Faculté des Sciences

Engel, M. S., Ceríaco, L. M., Daniel, G. M., Dellapé, P. M., Löbl, I., Marinov, M., ... & Zacharie, C. K. (2021). The taxonomic impediment: A shortage of taxonomists, not the lack of technical approaches. *Zoological Journal of the Linnean Society*, *193*(2), 381–387.

Espitalié, J., Laporte, J. L., Madec, M., Marquis, F., Leplat, P., Paulet, J., & Boutefeu, A. (1977). Méthode rapide de caractérisation des roches mères de leur potentiel pétrolier et de leur degré d'évolution. *Revue De L'institut Français Du Pétrole, 32*, 23–42.

Felhi, M. (2010). *Les niveaux intercalaires de la série yprésienne du bassin Gafsa-Métlaoui: Apports de la minéralogie des argiles et de la géochimie de la matière organique résiduelle à la reconstitution paléoenvironnementale* (pp. 82–84). PhD thesis, Univ. Sfax. Faculty of Sciences of Sfax.

Gallela, W. (2010). *Les sables quartzo-feldspathiques de la Tunisie centroméridionale: Sédimentologie, minéralogie et applications industrielles* (pp. 79–82). PhD thesis, Univ. Sfax. Faculty of Sciences of Sfax.

Gammoudi, A., Tlili, A., Essefi, E., El Feki, H., & Rigane, H. (2021). Contribution of the geochemical, physico-chemical, mineralogical, and statistical approaches to the reconstructing of the Holocene depositional environments along South-Eastern Tunisi. *Arabian Journal of Geosciences, 14*, 2029. https://doi.org/10.1007/s12517-021-08227-4

Gargouri, Z. (2011). Étude sédimentologique et radiochronologique des dépôts du domaine paralique dans le golfe de Gabès (sebkha El Guettiate–sebkha Dreîaa). These

de doctorat Université de Sfax. Faculté Des Sciences De Sfax, 204.

Gargouri, Z., & Zouari, K. (2019). Paleoenvironment Evolution of a Paralic System, El Guettiate and Dreïaa Sebkhas (Gulf of Gabès, Tunisia). In Patterns and Mechanisms of Climate, Paleoclimate and Paleoenvironmental Changes from Low-Latitude Regions: Proceedings of the 1st Springer Conference of the Arabian Journal of Geosciences (CAJG-1), Tunisia 2018 (pp. 85–88). Springer International Publishing.

Giraudi, C., Magny, M., Zanchetta, G., & Drysdale, R. N. (2011). The Holocene climatic evolution of Mediterranean Italy: A review of the continental geological data. *Holocene, 21*(1), 105–115.

Giraudi, C. (2005). Eolian sand in the peridesert northwestern Libya and implications for Late Pleistocene and Holocene Sahara expansion. *Palaeogeography, Palaeoclimatology, Palaeoecology, 218*, 161–173.

Goulden, M., Conway, D., & Persechino, A. (2009). Adaptation to climate change in international river basins in Africa: A review/adaptation au changement climatique dans les bassins fluviaux internationaux en Afrique: Une revue. *Hydrological Sciences Journal, 54*(5), 805–828. https://doi.org/10.1623/hysj.54.5.805

Janik, L. J., Merry, R. H., Forrester, S. T., Lanyon, D. M., Rawson, A., & Mars-avril. (2007). Rapid prediction of soil water retention using mid infrared spectroscopy. *Soil Science Society of America, 71*(2), 507–514.

Jaouadi, S., Lebreton, V., Bou-Roumazeilles, V., Guiseppe, S., Lakhdar, R., Boussoffara, R., Dezileau, L., Kallel, N., Mannai-tayech, B., & Combourieu-Nebout, N. (2016). Environmental changes, climate and anthropogenic impact in South-East Tunisia during the last 8 kyr. *Climate of the Past, 12*, 1339-e1359.

Kanbar, M., De Michele, F., Giudice, M. G., Desmet, L., Poels, J., & Wyns, C. J. H. R. (2021). Long-term follow-up of boys who have undergone a testicular biopsy for fertility preservation. *Human Reproduction, 36*(1), 26–39.

Koegel-Knabner, I., & Rumpel, C. (2018). Advances in molecular approaches for understanding soil organic matter composition, origin, and turnover: A historical overview. *Advances in Agronomy, 149*, 1–48.

Lafargue, E., Marquis, F., & Pillot, D. (1998). *Rock-Eval 6 applications in hydrocarbon exploration, production, and soils contamination studies* (pp. 421–437). Rev Instit Franç Pétrole.

Lakhdar, R. (2009). *Les sédiments holocènes et les tapis microbiens du littoral du Sud-Est de la Tunisie : sédimentologie et paléoenvironnements*. PhD, Université de Sfax.

Lakhdar, R., Soussi, M., & Talbi, R. (2021). Modern and Holocene microbial mats and associated microbially induced sedimentary structures (MISS) on the southeastern coast of Tunisia (Mediterranean Sea). *Quaternary Research, 100*, 77–97.

Lakhdar, R., Soussi, M., Ben Ismail, M. H., & M'Rabet, A. (2006). A Mediterranean Holocene restricted coastal lagoon under arid climate: Case of the sedimentary record of Sabkha Boujmel (SE Tunisia). *Palaeogeography, Palaeoclimatology, Palaeoecology, 241*, 177-e191.

Madejova, J., Keckés, J., Palkova, H., & Komadel, P. (2002). Identification of components in smectite/kaolinite mixtures. *Clay Minerals, 37*, 377–388.

Madéjova, J., & Komadel, P. (2001). Baseline studies of the clay minerals society source clays: Infrared methods. *Clays and Clay Minerals, 49*(5), 410–432.

Magny, M. (2004). Holocene climate variability as reflected by mid-European lake-level fluctuations and its probable impact on prehistoric human settlements. *Quaternary International, 13*, 65–79.

Magny, M., Peyron, O., Gauthier, E., Roueche, Y., Bordon, A., Billaud, Y., Chapron, E., Marguet, A., Magny, M., Peyron, O., Gauthier, E., Vanniere, B., Millet, L., & Vermot-Desroches, B. (2011). Quantitative estimates of temperature and precipitation changes over the last millennium from pollen and lake-level data at Lake Joux, Swiss Jura Mountains. *Quaternary Research, 75*, 45–54.

Marquer, L., Pomel, S., Abichou, A., Schulz, E., Kaniewski, D., & Van Campo, E. (2008). Late Holocene high resolution palaeoclimatic reconstruction inferred from Sebkha Mhabeul, Southeast Tunisia. *Quaternary Research, 70*, 240-e250.

Martín, M. G., Álvarez, A. P., Ordieres-Meré, J., Villalba-Díez, J., & Morales-Alonso, G. (2020). New business models from prescriptive maintenance strategies aligned with sustainable development goals. *Sustainability, 13*(1), 1–26.

Mats O. Molén (2024) Geochemical proxies: Paleoclimate or paleoenvironment?. *3*(1), 100238. https://doi.org/10.1016/j.geogeo.2023.100238

Mayewski, P. A., Rohling, E. E., Curt Stager, J., Karlen, W., Maasch, K. A., David Meeker, L., Meyerson, E. A., Gasse, F., van Kreveld, S., Holmgren, K., Lee-Thorp, J., Rosqvist, G., Rack, F., Staubwasser, M., Schneider, R. R., & Steig, E. J. (2004). Holocene climate variability. *Quaternary Research, 62*, 243–255.

Mohammad, Y. B., & Awadh, S. M. (2023). Geochemistry of Sabkhas in Abu Ghraib, Western Baghdad, Iraq. *The Iraqi Geological Journal*, 145–158.

Nash, D. J., & Meadows, M. E. (2012). *Quaternary environmental change in the tropics, chapter 4 Africa* (First Edition). John Wiley and Sons edition.

Ouaja, M., Slimane, N., & et Khila, A. (2013). Genèse et dynamique sédimentaire des dépôts désertiques de la région de Nefzaoua (sud-ouest de la Tunisie). Erosion éolienne dans les régions arides et semi-arides africaines : processus physiques, métrologie et techniques de lutte, 13.

Pacton, M., Fiet, N., & Gorin, G. E. (2007). Bacterial activity and preservation of sedimentary organic matter: The role of exopolymeric substances. *Geomicrobiology Journal, 24*(7–8), 571–581.

Pomel, S., Abichou, A., & Schulz, E. (2008). *La signification paléoimpluviométrique des sédiments de la sebkha Mhabeul (Sud-Est de la Tunisie)* (pp. 435–442). Presses Université Blaise Pascal.

Saikia, N. J., Bharali, D. J., Sengupta, P., Bordoloi, D., Goswamee, R. L., Saikia, P. C., & Borthakur, P. C. (2003). Characterization, beneficiation and utilization of a kaolinite clay from Assam, India. *Applied Clay Science, 24*(2003), 93–103. https://doi.org/10.1016/S0169-1317(03)00151-0

Schulz, E., Abichou, A., Hachicha, T., Pomel, S., Salzmann, U., & Zouari, K. (2002). Sebkhas as ecological archives and the

vegetation and landscape history of southern Tunisia during the last two millennia. *Journal of African Earth Sciences, 34*, 223-e229.

Shen, M., Xiong, W., Song, B., Zhou, C., Almatrafi, E., Zeng, G., & Zhang, Y. (2022). Microplastics in landfill and leachate: Occurrence, environmental behavior and removal strategies. *Chemosphere, 305*, 135325.

Sivakumar, S., Ravisankar, R., Raghu, Y., Chandrasekaran, A., & Chandramohan, J. (2012). FTIR spectroscopic studies on coastal sediment samples from Cuddalore District, Tamilnadu, India. *Indian J Adv Chem Sci, 1*, 40–46.

Srarfi, F., Tagourti, M. A., Tlig, S., & Slim Shimi, N. (2010). Influence de la separation granulométrique sur la composition des sédiments en métaux lourds de la lagune de bizerte (Tunisie). *Communication Sciences et Technologie*, N°8 janvier 2010.

Srarfi, F., Rachdi, R., Bol, R., Gocke, M. I., Brahim, N., & Slim-Shimi, N. (2019). Stream sediments geochemistry and the influence of flood phosphate mud in mining area, Metlaoui, Western south of Tunisia. *Environmental Earth Sciences, 78*, 1–13.

Tagorti, M. A. (1990). *Dynamique de couverture, genèse et évolution du complexe lagunaire Sebkhat Halk El Mengel et Sebkhat Assa El Jeriba (Sahel de Sousse)* (p. 162p). Doct. Spéc., Univ. Tunis II, Fac. Sc. Tunis.

Triki, H., Sun, Y., Zhou, Q., Biswas, A., Yıldırım, Y., & Alshehri, H. M. (2022). Dark solitary pulses and moving fronts in an optical medium with the higher-order dispersive and nonlinear effects. *Chaos, Solitons & Fractals, 164*, 112622.

Trabelsi, W. (2017). *Effet de l'activation acido-basique sur la minéralogie des argiles smectitiques crétacés éocènes de la Tunisie méridionale : Application à la purification de l'acide phosphorique* (p. 80). PhD thesis. Univ. Sfax. Faculty of Sciences of Sfax.

Terink, W., Immerzeel, W. W., & Droogers, P. (2013). Projections du changement climatique des précipitations et de l'évapotranspiration de référence pour le Moyen-Orient et l'Afrique du Nord jusqu'en 2050. *Revue Internationale De Climatologie, 33*(14), 3055–3072.

Truche C (2010) Caractérisation et quantification des minéraux argileux dans les sols expansifs par spectroscopie infrarouge aux échelles du laboratoire et du terrain. Planète et Univers [physics]. Université Paul Sabatier - Toulouse III. https://theses.hal.science/tel-00594021.

Van Cappellen, P. (2003). Biomineralization and global biogeochemical cycles. *Reviews in Mineralogy and Geochemistry, 54*(1), 357–381.

Viscarra Rossel, R. A., Walvoort, D. J. J., McBratney, A. B., Janik, L. J., & Skjemstad, J. O. (2006). Visible, near infrared, mid infrared or combined diffuse reflectance spectroscopy for simultaneous assessment of various soil properties. *Geoderma, 131*, 59–75.

Wanner, H., Beer, J., Bütikofer, J., Crowley, T. J., Cubasch, U., Flückiger, J., Goosse, H., Grosjean, M., Joos, F., Kaplan, J. O., Küttle, M., Müller, A. S., Colin Prentice, I., Solomina, O., Stocker, T. F., Tarasov Wagner, M., & Widmann, M. (2008). Mid- to Late Holocene climate change: An overview. *Quaternary Science Reviews, 27*, 1791–1828.

Warren, J. (2000). Dolomite: Occurrence, evolution and economically important associations. *Earth-Science Reviews, 52*, 1–81.

Yusuf, M. O. (2023). Bond characterization in cementitious material binders using Fourier-transform infrared spectroscopy. *Applied Sciences, 13*(5), 3353.

Zaîbi C, Carbonel P, Kamoun F, Azri C, Kharroubi A, Kallel N, Jedoui Y, Montacer M, Fontugne M (2011) Coast line evolution during the late Holocene in the Sebkha El Guettiate of Skhira (Gulf of Gabes, Tunisia) based on its ostracod and foraminifera fauna.

Zaïbi C, Kamoun F, Viehberg F, Carbonel P. Jedoui Y, Abida H, Fontugny M (2016) Impact of relative sea level and extreme climate events on the Southern Skhira coastline (Gulf of Gabes, Tunisia) during Holocene times: Ostracodes and foraminifera associations' response.

Zaibi, C., Carbonel, P., Kamoun, F., Fontugne, M., Azri, C., Jedoui, Y., & Montacer, M. (2012). Evolution of the Sebkha dreîaa (South-Eastern Tunisia, Gulf of Gabes) during the late Holocene: Response of ostracod assemblages. *Revue de Micropaléontologie, 55*, 83-e97.